

3C273 variability at 7 mm: Evidences of shocks and precession in the jet.

Pedro Paulo B. Beaklini¹

Zulema Abraham¹

¹*Instituto de Astronomia, Geofísica e Ciências Atmosféricas, Universidade de São Paulo.*

Rua do Matão 1226, 05508-090, São Paulo/SP, Brazil.

Released 2011 Xxxxx XX

ABSTRACT

We report 4 years of observations of 3C273 at 7 mm obtained with the Itapetinga Radiotelescope, in Brazil, between 2009 and 2013. We detected a flare in 2010 March, when the flux density increased by 50% and reached 35 Jy. After the flare, the flux density started to decrease and reached values lower than 10 Jy. We suggest that the 7 mm flare is the radio counterpart of the γ -ray flare observed by Fermi/LAT in 2009 September, in which the flux density at high energies reached a factor of fifty of its average value. A delay of 170 days between the radio and γ -ray flares was revealed using the Discrete Correlation Function (DCF) that can be interpreted in the context of a shock model, in which each flare corresponds to the formation of a compact superluminal component that expands and becomes optically thin at radio frequencies at latter epochs. The difference in flare intensity between frequencies and at a different times, is explained as a consequence of an increase in the Doppler factor δ , as predicted by the 16 year precession model proposed by Abraham & Romero, which has a large effect on boosting at high frequencies while does not affect too much the observed optically thick radio emission. We discuss other observable effects of the variation in δ , as the increase in the formation rate of superluminal components, the variations in the time delay between flares and the periodic behaviour of the radio light curve that we found compatible with changes in the Doppler factor.

Key words: (galaxies:) quasars: individual: 3C273

1 INTRODUCTION

Even though the launch of the Fermi Gamma-ray Space Telescope resulted in an unprecedented amount of data, which complemented the already known lower frequency spectral energy distribution (SED) of active galactic nuclei (AGNs), the actual emission process at each frequency is still under debate. There is no doubt that the radio emission has synchrotron origin, but the high energy X- and γ -rays can be attributed to different processes, like inverse Compton up scattering of low frequency photons, either of synchrotron origin (Synchrotron Self Compton, SSC), or external (External Compton, EC), or even hadronic processes initiated by relativistic protons (see review by Böttcher 2010).

Besides a quiescent or slowly varying emission, blazars present short duration high energy γ -ray flares with intensities that can differ in several orders of magnitude, even for flares in the same object. Similar but longer lasting flares are observed at infrared and radio frequencies, the latter associated with the appearance of relativistically beamed super-

luminal components in the parsec scale jets (Jorstad et al. 2001). As the radio emission, the γ -ray flux must be also relativistically beamed, to account for the short variability timescales and for the small optical depth for pair production (Mattox et al. 1993; Wehrle et al. 1998).

The superluminal components do not have the same apparent velocity and position angle in the plane of the sky (eg. Cotton et al. 1979), and in the case of 3C273, the systematic variation of these quantities were interpreted as due to jet precession, assuming ballistic motion for the components (Abraham & Romero 1999). The period detected was 16 years, which together with the black hole mass, suggested that the Bardeen-Peterson effect could be the origin of this precession (Caproni et al. 2004).

Considering only single dish observations, the radio emission of 3C273 was extensively monitored at different frequencies (Türler et al. 1999; Soldi et al. 2008). This long time coverage (almost 40 years) allowed statistical studies that revealed the existence of several periodicities, in-

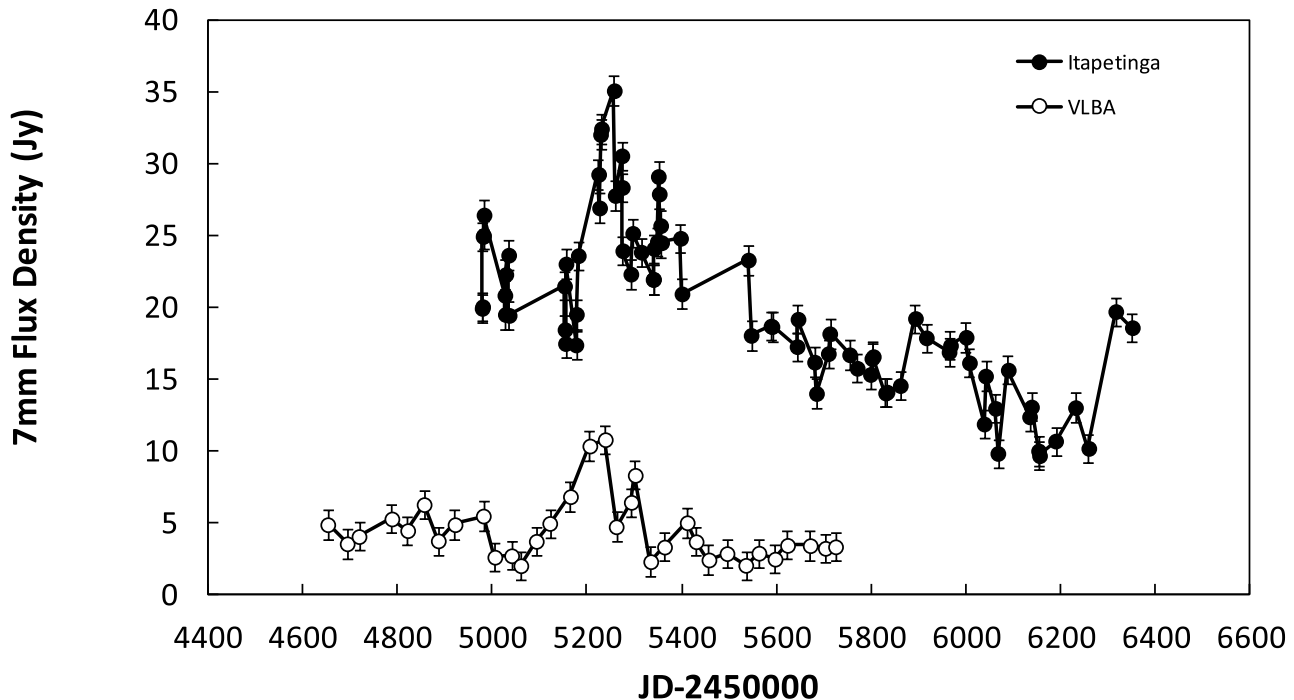


Figure 1. The 7 mm single dish light curve of 3C273 (this work) and the flux densities of the obtained with the VLBA by Marscher et al. (2012).

cluding 8 and 32 years (Fan et al. 2007; Zhang et al. 2010; Vol’vach et al. 2013).

The formation of the superluminal components was attributed to particle acceleration in shocks propagating along the relativistic jet (Marscher & Gear 1985; Hughes, Aller & Aller 1985; Spada et al. 2001; Marscher & Jorstad 2010; Hughes, Aller & Aller 2011), and their temporal evolution at different frequencies was extensively explored, (eg. Türler et al. 2000; Böttcher 2010). Since initially the shocked region is optically thick at radio frequencies, a delay between the maxima in the light curves at different frequencies is expected.

The detection of time delays is not easy, because the association of the flares at different frequencies is not unique, and even in the same source, each flare could have a different time delay. Before the Fermi era, a time delay of hundred days was detected in 3C273, between radio and infrared flares, with the infrared flare coming first (Clegg et al. 1983; Robson et al. 1983; Botti & Abraham 1988; Stevens et al. 1994, 1998).

Long time delays (1 to 8 months) between radio and γ -ray emission in Fermi blazars were measured comparing the light curves of 186 sources from the MOJAVE program (Lister et al. 2009) with the Fermi results (Pushkarev et al. 2010). In 3C279, a time delay of 6 months between the light curves was detected (Chatterjee et al. 2008). However, up to now there was no mention of time delay between radio and γ -rays in the literature for 3C273, although the relation between these frequencies was discussed in several occasions (Jorstad et al. 2001, 2012; Marscher et al. 2012).

In this paper we present 7 mm (43 GHz) single dish ob-

servations of 3C273 and associated the radio flare detected in 2010 March with the γ -ray flare observed by Fermi/LAT in 2009 September (Section 2). We discussed the time delay in terms of a shock model and interpreted the high intensity of the γ -ray flare as a consequence of an increase in the Doppler factor as predicted by the precession model of Abraham & Romero (1999) (Section 3). At last, in Section 4 we presented our conclusions.

2 OBSERVATIONS AND RESULTS

The observations of 3C273 at 7mm were made with the 13.7 m radome enclosed Itapetinga radio telescope, between 2009 and 2013. At this wavelength, the antenna half power beam width (HPBW) is about 2.4 arcmin and the radome transmission 0.68. The receiver, a room temperature K-band mixer, has a 1-GHz double side band (d.s.b) and a noise temperature of about 700 K. The calibration was made with a known temperature noise source and a room temperature load, which automatically corrects for atmospheric attenuation and radome absorption (Abraham & Kokubun 1992). The HII region SgrB2 Main was used as a primary flux calibrator. The method of observation consisted of scans in elevation and azimuth with an amplitude of 30 arcmin and 20s duration. The scans in each direction were averaged, a baseline was subtracted to eliminate the contribution of the atmosphere, and a Gaussian with the 7 mm HPBW was fitted to the remaining data to obtain the flux density; its central position was used to check the pointing accuracy.

The 7 mm data, obtained between 2009 May and 2013

Table 1. Days of Observations and flux density values

Date	JD-2450000	Flux Density (Jy)	Error (Jy)	Date	JD-2450000	Flux Density (Jy)	Error (Jy)
27/05/2009	4978	19.94	0.99	27/01/2011	5588	18.70	0.92
28/05/2009	4979	20.05	1.06	29/01/2011	5590	18.66	0.80
29/05/2009	4980	24.95	0.92	23/03/2011	5643	17.27	0.83
30/05/2009	4981	25.02	0.84	25/03/2011	5645	19.18	0.96
31/05/2009	4982	26.45	1.01	29/04/2011	5680	16.19	1.10
14/07/2009	5026	20.85	0.95	03/05/2011	5684	14.00	1.11
15/07/2009	5027	19.51	0.80	28/05/2011	5709	16.78	0.87
16/07/2009	5028	22.30	1.07	31/05/2011	5712	18.17	1.00
21/07/2009	5034	23.65	1.11	12/07/2011	5754	16.70	1.75
22/07/2009	5035	19.45	0.69	28/07/2011	5770	15.76	0.62
17/11/2009	5152	21.49	1.35	25/08/2011	5798	15.33	0.60
18/11/2009	5153	18.45	1.00	28/08/2011	5801	16.44	0.63
19/11/2009	5154	17.49	0.94	31/08/2011	5804	16.57	0.64
20/11/2009	5155	23.03	1.16	26/09/2011	5830	14.03	0.64
11/12/2009	5176	17.39	0.91	29/09/2011	5833	14.10	0.64
12/12/2009	5177	19.52	1.08	27/10/2011	5861	14.56	1.00
16/12/2009	5181	23.61	1.59	28/11/2011	5893	19.23	1.11
28/01/2010	5224	29.28	2.33	21/12/2011	5916	17.88	1.50
30/01/2010	5226	26.94	1.85	07/02/2012	5964	16.89	0.80
01/02/2010	5228	32.05	2.34	10/02/2012	5967	17.35	0.89
03/02/2010	5230	32.46	1.65	14/03/2012	6000	17.92	1.29
02/03/2010	5257	35.11	2.92	21/03/2012	6007	16.14	0.90
04/03/2010	5259	27.81	1.19	21/04/2012	6038	11.88	0.92
18/03/2010	5273	30.57	1.16	24/04/2012	6041	15.22	1.70
19/03/2010	5274	28.37	1.17	15/05/2012	6062	12.96	0.89
20/03/2010	5275	23.95	1.85	20/05/2012	6067	9.83	0.74
06/04/2010	5292	22.32	2.01	11/06/2012	6089	15.63	1.47
10/04/2010	5296	25.17	0.85	26/07/2012	6134	12.38	0.87
28/04/2010	5314	23.86	0.84	30/07/2012	6138	13.06	0.64
30/04/2010	5339	21.95	0.79	14/08/2012	6153	10.00	0.59
13/05/2010	5340	21.96	0.76	16/08/2012	6155	9.67	0.60
15/05/2010	5341	24.11	1.25	19/09/2012	6189	10.69	1.34
01/06/2010	5348	24.59	1.02	31/10/2012	6231	13.02	1.97
03/06/2010	5350	29.13	0.98	28/11/2012	6259	10.18	1.68
05/06/2010	5352	27.91	1.09	24/01/2013	6316	19.72	2.10
08/06/2010	5355	25.70	0.88	28/02/2013	6351	18.59	1.18
10/06/2010	5357	24.52	1.06	03/04/2013	6385	17.16	1.40
20/07/2010	5397	24.82	0.98	07/04/2013	6389	17.36	1.39
23/07/2010	5400	20.95	0.72	11/04/2013	6393	18.11	0.79
10/12/2010	5540	23.30	0.93	10/05/2013	6421	17.62	0.74
16/12/2010	5546	18.05	1.50	13/05/2013	6425	16.90	0.95

April, are presented in Table 1 and in the upper part of Fig. 1. In the first epoch of our monitoring, between 2009 and 2010, we detected a series of flares, the strongest with maximum flux density of 35.1 ± 2.9 Jy on 2010 March 2; in the second epoch, between 2011 and 2013, we detected a continuous decrease in the flux density, reaching the minimum of 9.8 ± 0.7 Jy on 2012 March 20. After this minimum, the flux density increased to the value that it had before the 2010 flare.

In total, our light curve has 82 days of observations, with two gaps of about 100 days, between July and November of 2009, and between July and December of 2010. Although the first gap coincided with the strong γ -ray flares reported by Abdo et al. (2010) in 2009 September and therefore, for which we do not have simultaneous 7 mm data, a large flare in radio was observed 6 months later, in 2010 March. The pattern of this radio flare is similar to that of the 2009 flare at γ -rays, as can be seen in Fig. 2, where we

present part our 7 mm light curve (upper part) and the γ -ray light curve (lower part) from the Fermi Space telescope¹ binned in 5 days intervals, with the time axis displaced by 150 days relative to the 7 mm time axis, so that the flares at the two different wavelengths became aligned.

Since the gap in our light curve does not allow us, without any other information, to affirm that the 2010 March radio flare is correlated with the 2009 September γ -ray flare, we analysed the 7 mm VLBA light curve of the compact core (Jorstad et al. 2012; Marscher et al. 2012) shown in the lower part of Fig. 1². The VLBA flux density does not show

¹ http://fermi.gsfc.nasa.gov/ssc/data/access/lat/mssl_c/

² Marscher et al. (2012) reported the flux density of 3C273 relative to the peak value of the light curve. To calculate the light curve in Jy, we used the peak value presented in the website of Boston University gamma-ray blazar monitoring program: <http://www.bu.edu/blazars/VLBAproject.html>

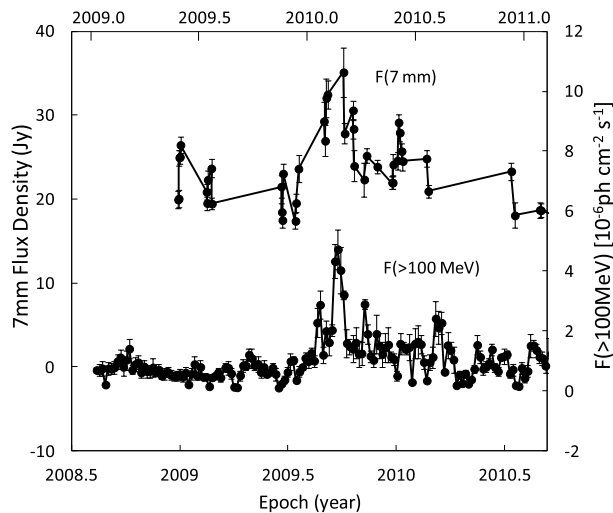


Figure 2. 7 mm and γ -ray light curves of 3C273, with time given in the upper and lower axis, respectively. The origin of the radio time axis was shifted by 170 days, to show the similarity between the flares at both frequencies.

any increase in intensity at the epoch of the γ -ray flare, instead of that, it was lower than at other epochs, while it reached its maximum value in 2010 March, at the same time as the Itapetinga light curve. We must emphasize the similarity between the two light curves, indicating that the 7 mm single dish observations reflect mainly the core variability. Furthermore, the VLBI images reported by Jorstad et al. (2012) do not present any strong variation in the flux density of the superluminal components at the epoch of the gamma ray flare, also in agreement with our observations.

Finally, we used the DCF (Discrete Correlation Function) to verify statistically the correlation between the 7 mm and γ -ray flares and to compute the correct time delay. The DCF is a simple test which calculates the correlation between two light curves without interpolating or creating data; the maxima indicate the time delays (Edelson & Krolik 1988). To calculate the DCF, we used the Itapetinga (46 points) and the Fermi light curve (758 points) shown binned in Fig. 2, because the rest of the light curves are not necessarily correlated. In Fig. 3 we presented the DCF that shows a wide maximum at delays between 120 and 170 days, meaning that the radio flare occurred after the γ -ray flare.

3 DISCUSSION

3.1 Flare intensities and the beaming factor

The first flare detected in 3C273 and monitored at different wavelengths (between $100\mu\text{m}$ and 8.9 mm) was reported by Clegg et al. (1983) and Robson et al. (1983). This flare reached the peak first at the higher frequencies and then propagated to millimeter wavelengths. In the attempt to explain this behaviour, Marscher & Gear (1985) proposed a model in which a shock wave propagates in the relativistic jet and evolves through three different phases of energy loss: Compton, synchrotron and adiabatic. The time delay

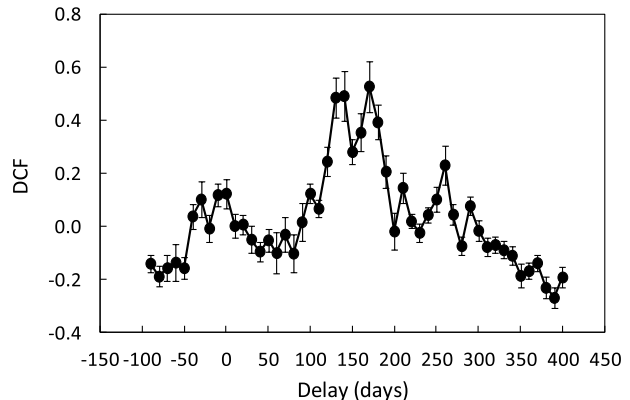


Figure 3. Results of the Discreted Correlation Function: the upper graph corresponds to the correlation of the real radio and γ -ray data, the lower corresponds to the correlation of simulated radio data with the real γ -ray light curve.

between the peak at different frequencies is a consequence of opacity, since the shock becomes optically thin at the lower frequencies as the component expands. In this model, the X-ray and infrared flares should precede the radio flare with timescale of months and in fact, the counterpart at 22 GHz of the infrared 1983 flare probably occurred 290 days later as proposed by Botti & Abraham (1988).

Stevens et al. (1994) detected typical time delays of about 100 days between flares at 37 and 90 GHz in 17 sources monitored by Aller et al. (1985) and in 3C273, Stevens et al. (1998) reported time delays between the frequencies of 375 and 4.8 GHz. In all these situations, the time delay can be explained by the shocked jet models (Marscher & Gear 1985; Hughes, Aller & Aller 1985) and their generalizations (Marscher 1990; Marscher et al. 1992; Stevens et al. 1996; Türler et al. 2000; Sokolov et al. 2004). Time delays even higher were predicted by Türler et al. (2000) between radio and infrared wavelengths, with the flare at high energy always coming first.

Before Fermi Gamma-ray Space Telescope started to operate, there was no much information about variability behaviour at γ -rays. EGRET, on board of GRO detected γ -rays of energies above 100 MeV with an average value between 1991 and 1995 of $(1.5 \pm 0.2) \times 10^{-7}$ photons $\text{cm}^{-2}\text{s}^{-1}$, while Collmar et al. (2000) reported the largest flare observed with this instrument with a duration at least of 30 days and a flux density of $(7.6 \pm 0.2) \times 10^{-7}$ photons $\text{cm}^{-2}\text{s}^{-1}$.

Chatterjee et al. (2012) analysed the variability of six sources at the infrared, including 3C273, and found a positive correlation with the flares detected by Fermi/LAT at γ -rays with an upper limit of three days for the time delays. Even when a delay is detected, as in 3C279, it was not higher than a few days (Hayashida et al. 2012). Considering the short time delays between the flares at these wavelengths, we interpreted that the 7 mm flares detected in 2010 March as the radio counterpart of the γ -ray flares detected by Fermi in 2009 September, in the same way as other radio flares were interpreted as radio counterparts, delayed by several months, of infrared flares (Botti & Abraham 1988; Stevens et al. 1994, 1998; Türler et al. 2000).

As discussed in Section 2, VLBI observations reported

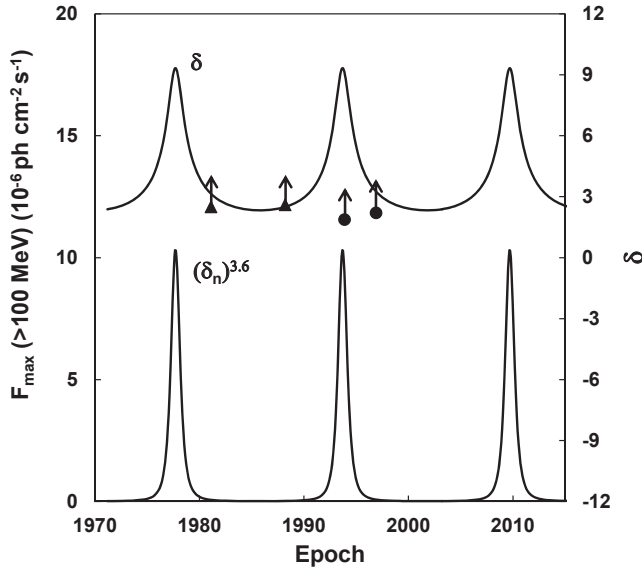


Figure 4. Doppler factor δ and beaming factor of the γ -ray emission $(\delta_n)^{3.6}$, as a function of time, according to a 16 y precessing jet model, described in the text. The beaming factor (δ_n) was normalized to match the amplitude of the largest γ -ray flare. Full triangles and circle are lower limits imposed to δ by X- and γ -ray observations, as described in Abraham & Romero (1999).

by Jorstad et al. (2012) show the appearance of four new superluminal components, ejected from the core between 2009.5 and 2010.5, at epochs coincident with the occurrence of the strong γ -ray flares. These coincidences also favours the shock model. However the high intensity of the γ -ray flares compared to the moderate intensity of the radio flares still needs elucidation; the change of the beaming factor as a consequence of jet precession, as proposed by Abraham & Romero (1999) seems to be a good explanation, as discussed below.

Both the radio and γ -ray emission must be boosted if the angle between the emitting region and the line of sight is small, but the effect in the flux density $S(\nu, \delta)$ is different at different frequencies, because in the observer reference frame:

$$S(\nu, \delta) \propto \delta^{(p+\alpha)} \nu^{-\alpha}, \quad (1)$$

where δ is the Doppler factor:

$$\delta = \frac{1}{\Gamma(1 - \beta \cos \theta)}, \quad (2)$$

and Γ the Lorentz factor:

$$\Gamma = \frac{1}{(1 - \beta^2)^{1/2}}, \quad (3)$$

β is the bulk jet velocity, θ the angle between the jet direction and the line of sight, α the spectral index and, $p = 2$ for a continuous jet and $p = 3$ for discrete components.

For 3C273, the spectral index in the γ -ray region of the spectrum is $\alpha > 1$, while in the radio region, for the newly formed optically thick components until it becomes optically thin $\alpha \sim -2$. Therefore, an increase in the Doppler factor will have a strong effect in the flare emission at γ -rays, while would barely affect the observed radio flux density. An increase in δ by a factor 3 or 4 seems to be a promising

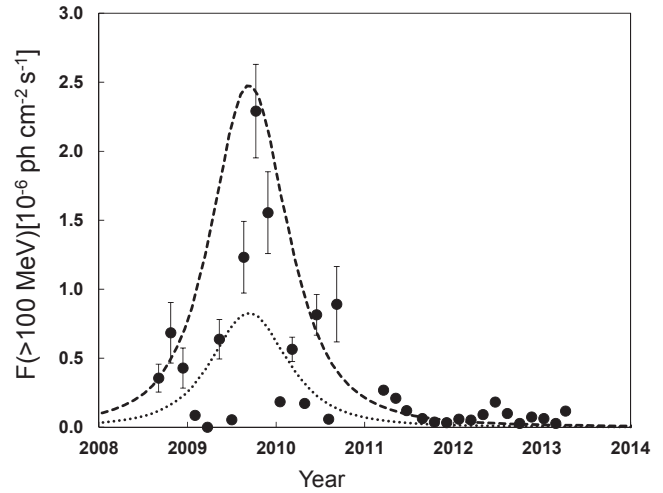


Figure 5. Fermi γ -ray light curve binned in 50 days (points) after discounting the minimum flux value from the data, which is of the order of the upper detection limit of the EGRET observations (Hartman et al. 1999). The dashed line represents the flux of an arbitrary average flare at different epochs due to beaming, the dot line represents the same for a flare with an intrinsic intensity equal to 1/3 of the average value.

explanation for the relative intensities of the flares at these two frequencies.

Periodic changes in the Doppler factor of 3C273 were predicted by Abraham & Romero (1999), as the result of changes in the angle between the jet direction and the line of sight, due to precession. The model was based on differences in the apparent superluminal velocities of components ejected at different epochs and in their position angles in the plane of the sky, and resulted in a precession period of 16 years. During each cycle the model predicts a variation of a factor of three in δ , and the maximum approach between the jet and the line of sight to occur in 2010, when the boosting was maximum. Minimum values for the Doppler factor were obtained using limits imposed by early X- and γ -ray observations (Abraham & Romero 1999; Collmar et al. 2000). We therefore calculated the beaming factor for the γ -ray photon flux density $\delta^{p+\alpha+1}$ as a function of time, using $p = 2$ and $\alpha + 1 = 1.6$ (Abdo et al. 2010), and the values of δ as a function of time obtained from a precession model with a period of 16 years, an opening angle of the precession cone of 4° , an angle between the cone axis and the line of sight of 10° and a Lorentz factor $\Gamma = 13$. This model fits the superluminal velocities of the jet components identified by Abraham et al. (1996); Lister et al. (2009); Jorstad et al. (2012). The Doppler and normalized beaming factor are presented in Fig. 4.

To compare the intensity of the γ -ray flares at different epochs we binned the γ -ray flux in intervals of 50 days, to obtain an error comparable to that of the light curve presented by Collmar et al. (2000); the large time bin also eliminates the small timescale variations. The results are presented in Fig. 5 where the dashed line represents the flux that an arbitrary average flare will have at different epochs due to beaming, and the dot line represents the same for a flare with an intrinsic intensity equal to 1/3 of the average. The

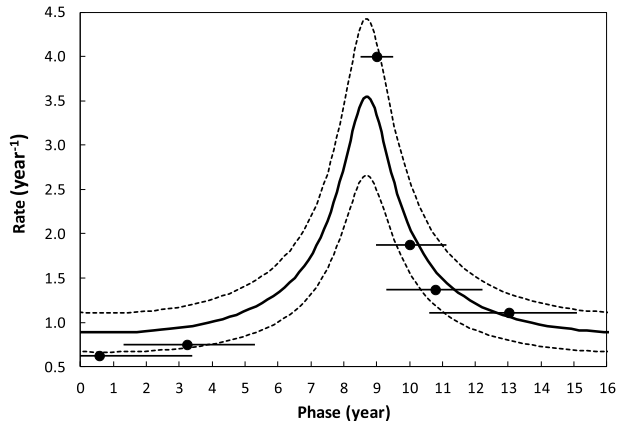


Figure 6. Ejection rate obtained from de precession model of components during the 16 year period. The dashed line represents a fluctuation of 25% in the rate, while the dots represents the observed rate. The phase 0 of the cycle was 1985 and the error bars represents the epoch used to determined the rate.

Table 2. Ejection Rate for superluminal components

number of components	rate (year ⁻¹)	epoch	reference
4	4.0	2009.5-2010.5	Jorstad et al. (2012)
4	1.4	1994.3-1997.2	Lister et al. (2009)
4	1.9	1996.1-1994	Homan et al. (2001)
5	0.8	1979.6-1984.1	Türler et al. (1999)
3	1.1	1986.3-1990.3	Türler et al. (1999)
3	0.6	1983.6-1988.4	Abraham et al. (1996)

low points values between 2009 and 2011 show the epochs with no flares.

Changes in the Doppler factor have other observable consequences. The first is the reduction in the time scale at the observer reference frame by a factor $\delta/\delta_{\text{ref}}$, where δ_{ref} is the Doppler factor at a given reference time. A reduction in the time scale would imply in the increase in the ejection rate of superluminal components, and in fact, Jorstad et al. (2012) reported the ejection of four components coincident with the strong γ -ray flares, while the average rate of ejection is 0.7 y^{-1} , as can be seen in Lister et al. (2009b).

In Fig 6 we show the ejection rate variability as a consequence of the time contraction during one precession cycle. Naturally, the intrinsic rate is not exactly the same every year and the fluctuations are also amplify by the Doppler factor during its maxima value. In the figure, the dashed lines represent fluctuation of 25% in the intrinsic rate at the source frame. It is not easy compare the predicted rate with the observational data because the ejection time of the components is not an observed quantity, and it is necessary to compute the component kinematics. The observed ejection rates were obtained using different works, they are presented in table 2 and shown by dots in Fig. 6, with error bars that indicate the interval at which the rate was obtained. We only used time intervals smaller than five years, and those in which the components were close to the core to guarantee that short lived components were not missed.

The second consequence of a change in δ is its effect on

the time delay τ between the radio and γ -ray flares. According to the shock model of Marscher & Gear (1985):

$$\tau(\delta, \nu) = \frac{R'(\nu')(1+z)}{\Gamma \delta c}, \quad (4)$$

where R' is the distance to the origin of the shock at which the source becomes optically thin at the frequency ν' , both measured in the source reference frame, z is the redshift and c the speed of light. If the source is already in the adiabatic energy lose phase:

$$R'(\nu') \propto (\nu')^{-\omega} \quad (5)$$

where $\omega = (3s + 12)/(7s + 8)$, and $s = 1 - 2\alpha$ is the index of the electron energy distribution.

Since $\nu' = \nu/\delta$, we obtain from equations (4) and (5):

$$\tau(\delta, \nu) = \tau(\delta_{\text{ref}}, \nu) \left(\frac{\delta}{\delta_{\text{ref}}} \right)^{(\omega-1)} \quad (6)$$

In the optically thin regime $\alpha \sim -0.7$, resulting in $\omega = 0.77$. For $\delta/\delta_{\text{ref}}$ equal to 3 or 4, the ratio $\tau(\delta, \nu)/\tau(\delta_{\text{ref}}, \nu)$ will be 0.78 and 0.73, respectively.

To evaluate the expected time delay $\tau(\delta, \nu)$ between the 7 mm and γ -ray flare, we use as a reference the flare that occurred in August 1995, and was detected at wavelengths ranging from 0.8 mm to 6.25 cm (Stevens et al. 1998). Since there are no γ -ray observation of this event, we assume that the maximum at 0.8 mm coincided with the origin of the flare, resulting in a time delay at 7 mm of 234 days, which gives $\tau(\delta, \nu) = 182$ or 170 days for $\delta/\delta_{\text{ref}}$ equal to 3 or 4, respectively, which agrees very well with the observed delay.

3.2 The precession model and the historic light curve

Since the radio variability is mainly due to the outbursts produced by the appearance of new jet components, the radio light curve should not be too much affected by the periodic Doppler variation, as discussed in the previous subsection. Furthermore, the formation of new components is not necessarily periodic, and in fact, the historic light curve compiled by Soldi et al. (2008) shows maxima and minima that do not seem to follow a periodic pattern, instead of that, they occur with different intensities and time intervals. However, the ejection rate of these components and their temporal evolution are dependent of the Doppler factor and can introduce a modulation in the radio light curve.

To verify the existence of periods, we used two different statistical test: Stellingwerf and Structure Function. Unfortunately, to detect a 16 year periodicity it is necessary a long time coverage for the light curve; for example, in 20 year interval only one cycle was completed, which turns the 16 year periodicity detection impossible. However, 3C273 is one of the best monitored radio sources in the sky, and the historic data covers 37 years at some frequencies (Soldi et al. 2008). The Stellingwerf method is not adequate to detected periodicities higher than 1/5 of the total time coverage, and it could not reveal the 16 year period without 80 years of radio observations. However, it can be very useful to identify possible resonant periodicities, as the 8 year periodicity detected in many works with other methods (Fan et al. 2007; Vol'vach et al. 2013).

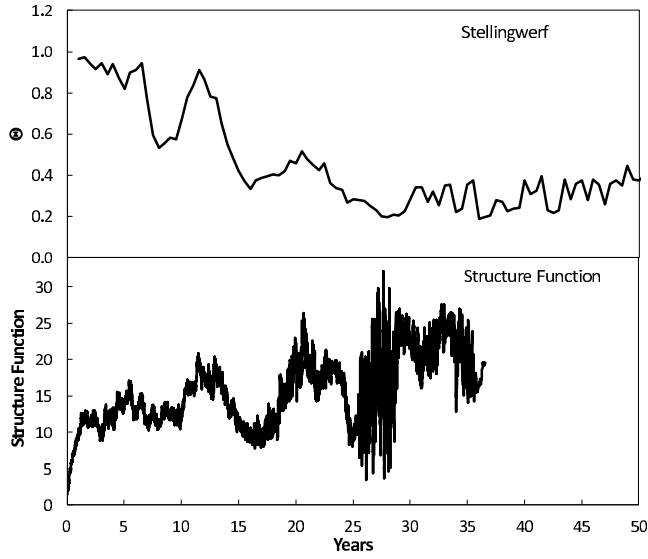


Figure 7. Upper part: Stellingwerf method result, which indicate a periodicity of 8 years. Lower part: Structure Function results, which indicate a periodicity of 16 years.

The Stellingwerf method (Stellingwerf 1978) divides the sample in m groups, following a phase vector given by:

$$\phi_i = \frac{t_i}{P} - \left[\frac{t_i}{P} \right], \quad (7)$$

where P is the guessed periodicity, t_i is the time of observation and the bracket means the integer part. For a given P , the Square Deviation of the flux density in each group is computed and the sum of all Square Deviations is divided by the total Square Deviation of the sample. The result of this fraction is defined as θ , and it will be minimum when the guessed periodicity is the real one. The minimum in the θ versus period curve will be deeper when m is higher, however, m can not be excessively high to allow a reliable statistics for each group; in our work we choose $m = 20$.

The Structure Function (SF) is a simply way to verify how much the intensity varies after a given time ξ and is given by:

$$SF(\xi) = \langle [I(t+\xi) - I(t)]^2 \rangle, \quad (8)$$

where I is the intensity at time t and $I(t+\xi)$ is the intensity after a time delay ξ . If there is indeed a periodicity T , when for $\xi = T$, there will be a minima in the SF curve.

Considering the different wavelengths presented in the historic data reported by Soldi et al. (2008), we choose the 37 GHz light curve to discuss the results of both methods, because it is the nearest frequency to our observations. However, we performed the tests at the other radio frequencies and the result are very similar, as already noted by Vol'vach et al. (2013). The 37 GHz data started at 1970 and ended at 2006, which gives a time coverage of almost 37 years; it is one of the frequencies with more observations days.

The result of the statistical tests are present in Fig. 7, the Stellingwerf method in the upper part and Structure Function in the lower part. The result of the Stellingwerf method shows a prominent minimum at 8 years, and a beginning of an even deeper minimum at 16, before the

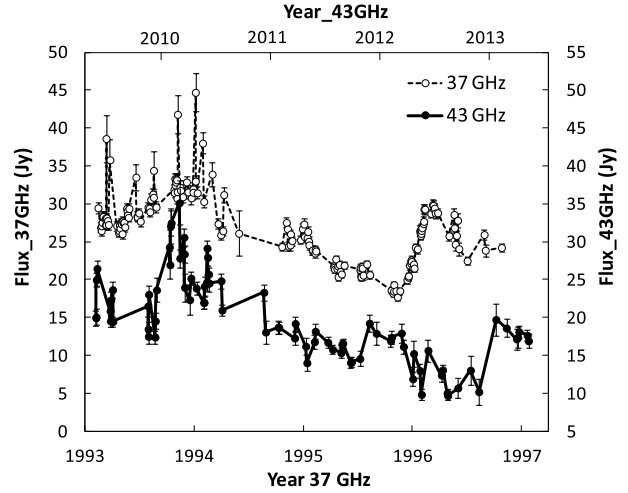


Figure 8. 37 GHz variability obtained between 1993 and 1997 (Soldi et al. 2008) and the 43 GHz variability obtained in this work, between 2009 and 2013. Both light curve show the same variability behaviour.

appearance of oscillations that are the consequence of insufficient time coverage. The significance of the minima is obtained applying the F-test, where $f = (1 - \Theta)/\Theta$, needs to be higher than 0.25 (Kidger et al. 1992), condition satisfied for the 8 year minimum, where $f = 0.86$. We interpreted this detection, also found Vol'vach et al. (2013) using Fourier Analysis, as a resonance of the 16 years precession period. The 16 year minimum also presents a high f value, however, as pointed out above, only the first period is inside the limit of what can be detected by the Stellingwerf method.

The SF intensity variation does not show any minima around 8 years, but shows a wide minimum around 16 years. The large width, which represents an imprecision in the detection of about 2 years, can be attributed to the small time coverage and to the fact that the formation of new components in the jet is not a strictly periodic phenomena. The result of both tests are consistent with the 16 years precession model, because the Stellingwerf method is efficient to detected the 8 year resonance while the SF reveals only the 16 year period.

Based on the statistical results, we compared the 43 GHz light curve obtained between 2009 and 2013, with that at 37 GHz, obtained 16 years earlier (Soldi et al. 2008), as shown in Fig. 8. Besides the 7 Jy difference in flux density, due to the difference in frequencies, both light curves show the same variability pattern, with the same long decrease in flux density that lasted for two years. Again, the individual oscillations do not match very well, as expected from the fact that the radio outbursts are not strictly periodic.

4 CONCLUSION

We presented the results of four years monitoring of 3C273 at 7 mm. During this period we detected a flare in 2010 March, that we interpreted as the radio counterpart of the extremely intense γ -ray flare observed by Fermi/LAT in

2009 September delayed by approximately 170 days. This delay can be understood in the context of the shock model in which the electrons are accelerated in a shock that propagates along the jet, originating the γ -ray flare through the Inverse Compton process and later the radio flare, when the shock turns optically thin at this lower frequency.

We explained the very high intensity of the γ -ray flare compared to previous ones as the consequence of boosting, produced by an increase in the Doppler factor by 3 or 4. The intensity of the radio emission, on the other hand, would not be affected, because the source was optically thick at these frequencies. A periodic variation of the Doppler factor was predicted by the precession model of Abraham & Romero (1999) for the jet of 3C273. The precessing period was 16 years and the parameters of the precessing jet used in the present work were: opening angle of the precession cone of 4° , angle between the cone axis and the line of sight of 10° and Lorentz factor $\Gamma = 13$.

Other observable consequences of the variation of the Doppler factor are the increase in the rate of superluminal ejections, which was confirmed by the work of Jorstad et al. (2012), and its effect on the time delay between flares at different frequencies, which was also compatible with the observations.

Although the Doppler factor does not affect the radio flux density, it modulates the radio light curve, as a consequence of the difference in the ejection rate of jet components and their temporal evolution. The Stellingwerf method and the Structure Function, calculated from the 37 GHz historic light curve, covering almost 40 years, revealed the existence of 8 and 16 year periodicity. We interpreted the first one, only detected by the Stellingwerf method, as a resonance of the 16 year period. Moreover, the variability pattern detected between 2009 and 2013 has the same trend than that detected 16 years earlier at 37 GHz.

ACKNOWLEDGMENTS

We are grateful to the Brazilian research agencies FAPESP and CNPq for financial support. This study makes use of 43 GHz VLBA data from the Boston University gamma-ray blazar monitoring program (<http://www.bu.edu/blazars/VLBAproject.html>), funded by NASA through the Fermi Guest Investigator Program. This research has made use of data from the MOJAVE database that is maintained by the MOJAVE team (Lister et al., 2009, AJ, 137, 3718).

REFERENCES

- Abdo, A. A., et al. 2010, ApJ, 714, L73
 Abraham, Z., Carrara, E. A., Zensus, J. A., & Unwin, S. C. 1996, A&AS, 115, 543
 Abraham, Z., & Kokubun, F. 1992, A&A, 257, 831
 Abraham, Z., Carrara, E. A., Zensus, J. A., & Unwin, S. C. 1996, A&AS, 115, 543
 Abraham, Z., & Romero, G. E. 1999, A&A, 344, 61
 Aller, H. D., Aller, M. F., Latimer, G. E., & Hodge, P. E. 1985, ApJS, 59, 513
 Böttcher, M., 2010, in Proceedings of the Workshop "Fermi meets Jansky: AGN in Gamma Rays", ed. T. Savolainen, E. Ros, R. W. Porcas, & J.A. Zensus, (Max-Planck-Institut für Radioastronomy, Bonn, Germany), 41
 Böttcher, M., Dermer, C.D., 2010, ApJ, 711, 445
 Botti, L. C. L., & Abraham, Z. 1988, AJ, 96, 465
 Caproni, A., Mosquera Cuesta, H. J., & Abraham, Z. 2004, ApJ, 616, L99
 Chatterjee, R., Jorstad, S. G., Marscher, A. P., et al. 2008, ApJ, 689, 79
 Chatterjee, R., Bailyn, C. D., Bonning, E. W., et al. 2012, ApJ, 749, 191
 Clegg, P. E., et al. 1983, ApJ, 273,
 Collmar, W., Reimer, O., Bennett, K., et al. 2000, A&A, 354, 513
 Cotton, W. D., Counselman, C. C., III, Geller, R. B., et al. 1979, ApJ, 229, L115
 Edelson, R., Krolik, J., 1988, ApJ, 333, 646
 Fan, J. H., Liu, Y., Yuan, Y. H., et al. 2007, A&A, 462, 547
 Hartman, R. C., Bertsch, D. L., Bloom, S. D., et al. 1999, ApJS, 123, 79
 Hayashida, M., Madejski, G. M., Nalewajko, K., et al. 2012, ApJ, 754, 114
 Homan, D. C., Ojha, R., Wardle, J. F. C., et al. 2001, ApJ, 549, 840
 Hughes, P. A., Aller, H. D., Aller, M. F., 1985, ApJ, 298, 301
 Hughes, P. A., Aller, M. F., Aller, H. D., 2011, ApJ, 735, 81
 Jorstad, S.G., Marscher, A.P., Mattox, J.R., Wehrle, A.E., Bloom, S.D., Yurchenko, A.V., 2001, Ap&SS, 134, 181
 Jorstad, et al., 2012, in High Energy Phenomena in Relativistic Outflows III, Intern. Jour. Mod. Phys. Conference Series 8, 356
 Kidger, M., Takalo, L., & Sillanpaa, A. 1992, A&A, 264, 32
 Lister, M. L., et al. 2009, AJ, 137, 3718
 Lister, M. L., Cohen, M. H., Homan, D. C., et al. 2009, AJ, 138, 1874
 Marscher, A. P., & Gear, W. K. 1985, ApJ, 298, 114
 Marscher, A. P. 1990, Parsec-scale radio jets, 236
 Marscher, A. P., Gear, W. K., & Travis, J. P. 1992, Variability of Blazars, 85
 Marscher, A. P., Jorstad, S. G., Agudo, I., MacDonald, N. R., & Scott, T. L. 2012, arXiv:1204.6707
 Marscher, A., Jorstad, S., 2010, in Proceedings of the Workshop "Fermi meets Jansky: AGN in Gamma Rays", ed. T. Savolainen, E. Ros, R. W. Porcas, & J.A. Zensus, (Max-Planck-Institut für Radioastronomy, Bonn, Germany), 1
 Mattox, J. R., Bertsch, D.L., Chiang, J. et al., 1993, ApJ, 410, 609
 Pushkarev, A. B., Kovalev, Y. Y., & Lister, M. L. 2010, ApJ, 722, L7
 Robson, E. I., et al. 1983, Nature, 305, 194
 Soldi, S., Türler, M., Paltani, S., et al. 2008, A&A, 486, 411
 Sokolov, A., Marscher, A. P., & McHardy, I. M. 2004, ApJ, 613, 725
 Spada, M., Ghisellini, G., Lazzati, D., Celotti, A., 2001, MNRAS, 325, 1559
 Stellingwerf, R. F. 1978, ApJ, 224, 953

- Stevens, J. A., Robson, E. I., Gear, W. K., et al. 1998, ApJ, 502, 182
- Stevens, J. A., Litchfield, S. J., Robson, E. I., et al. 1996, ApJ, 466, 158
- Stevens, J. A., Litchfield, S. J., Robson, E. I., et al. 1994, ApJ, 437, 91
- Türler, M., Courvoisier, T.J.-L., Paltani, S., 2000, A&A, 361, 850
- Türler, M., Paltani, S., Courvoisier, T. J.-L., et al. 1999, A&AS, 134, 89
- Vol'vach, A. E., Kutkin, A. M., Vol'vach, L. N., et al. 2013, Astronomy Reports, 57, 34
- Wehrle, A.E., Pian, E., Urry, C.M., Maraschi, L., McHardy, I.M. et al., 1998, ApJ, 497, 178
- Zhang, H., Zhao, G., Zhang, X., & Bai, J. 2010, Science in China G: Physics and Astronomy, 53, 252